Master's Thesis

Label-free Histopathological Vessel Imaging Based on Serial Optical Coherence Tomography

Songyee Baek

Department of Biomedical Engineering

Graduate School of UNIST

2017

Label-free Histopathological Vessel Imaging Based on Serial Optical Coherence Tomography

Songyee Baek

Department of Biomedical Engineering

Graduate School of UNIST

2017

Label-free Histopathological Vessel Imaging Based on Serial Optical Coherence Tomography

A thesis/dissertation
submitted to the Graduate School of UNIST
in partial fulfillment of the
requirements for the degree of
Master of Science

Songyee Baek

06. 26. 2017 of submission
Approved by

_____

Advisor
Woonggyu Jung

Label-free Histopathological Vessel Imaging Based on Serial Optical Coherence Tomography

Songyee Baek

This certifies that the thesis/dissertation of Songyee Baek
is approved.

06/ 26/ 2017

signature

_____

Advisor : Woonggyu Jung

signature

_____

Hyugmoo Kwon : Thesis Committee Member

signature

_____

Jihyeon Kim : Thesis Committee Member

Contents

LIST OF FIGURES

Abstract

Blood vessels are the tubes that exchange nutrients and waste products from our bodies and have a dense network of large vessels to capillaries. If the network of these ducts is lost its functions due to or ischemia, it becomes a serious problem leading to complications of various organs. There are macroscopic or microscopic ways of imaging these vessels. However, the highest resolution achievable is beyond the scale of the cell, so their application remains in large-scale organ structures and functions. Moreover, the microscopic method can obtain a precise image of a cell, but the depth of the image is only a few hundred microns, so it can hardly be extended to study the function or structure of the organ because it is hardly light. Optical Coherence Tomography is a potential imaging modality that makes it possible for achieving the cross-sectional image non-invasively in high resolution of sub-micron. Relatively, however, OCT has a limitation in penetration depth, thus has suffered from reconstructing the tissue in 3D when examining pathological studies. Therefore, we utilize the continuous cutting method by simultaneously obtaining the structure and function using the advantages of the macroscopic imaging technique and the advantage of the microscopic imaging technique.

In this study, we would like to propose a block face imaging technique combined with OCT. It has very detailed pathological information to distinguish between normal and diseased models. So, other organs such as kidneys, spinal cord, and liver can also be obtained images. Through reconstructed in both morphology and vascular network by using Serial Optical Coherence Tomography, our results are expected to have high potential to identify the morphological changes in other normal and disease models.

Keyword: Acute Kidney Injury (AKI), Chronic Kidney Disease (CKD), Vascular network, Renal morphology, Spinal cord morphology, Serial Optical Coherence Tomography (SOCT)

Chapter 1. Introduction

The vessels are the thin tube that carries blood. It divided into arteries, veins, and capillaries. Also, its formation can generate a number of different processes (1, 2). It plays a significant role in accepting the carbon dioxide and waste products that are excreted by peripheral cells and tissues. An artery is a tube that carries oxygen and nutrient-containing blood from the heart to the body, gradually tapering to capillary vessels, and the substance exchanged with the tissues, then the blood collects back into the vein and returns to the heart. These macroscopic large blood vessels close to the heart of our body are relatively well known in the disease, so the treatment and preventive measures are well specified. But an imbalance in the growth of blood vessels contributes to the pathogenesis of numerous disorders. The blood vessels and organs far away from the heart have an organic relationship with each other, especially the blood vessels in the organs, which provide nutrients to the organs, collect waste products, and provide power to move to the micro-capillaries of our bodies. However, such vessel diseases in the organs are difficult to access, and imaging and mechanism studies are also difficult to carry out simultaneously.

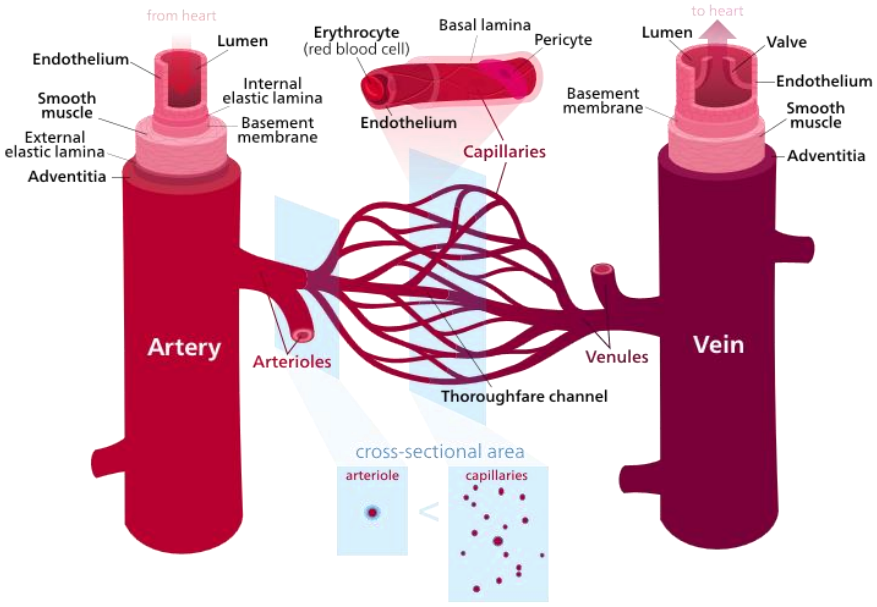

Figure 1-1. Illustration of blood vessels structure. Largely, it divided into arteries, veins, and capillaries.

Kidney disorder is a complicated and increasing matter of overall countries, which include acute kidney injury and chronic kidney disease. These two groups of diseases can observe an imbalance in the relationship between blood vessels and organs. Also, morbidity and mortality of renal disorder patients are considered to exceed 50 %, and these rates have not been declined during several decades (3, 4). Lots of nephrologists have tried to figure out the morphological change of kidney structure by various

interstitial protein and other immunological mechanism related AKI and CKD. However, there has been the inherent limitation to make a direct visualization on kidney structural change with conventional analytic techniques have been studied for specific sections. In addition to there is no specific imaging tool that is showing both structural and inner components. Optical tissue imaging provides potential advantages in distinguishing different structures according to their chemical composition. Because tissue is an exceedingly scattering medium for electromagnetic waves in an optical spectral range, methods that try to form images from light passing through tissue fall under two categories—ballistic (minimally scattered) optical microscopy and diffuse (multi-scattered) optical tomography. Optical coherence tomography (OCT) is a 3-dimensional high-resolution imaging modality (5) that calculates the delay of light to generate images (6, 7). Although the light scattering properties of biological sample typically limit light penetration to less than 2 mm, these imaging depth has proven sufficient to provide valuable information about tissue pathology in some biomedical fields (8). Also, OCT imaging enabled visualization of the morphology of blood vessels. Three-dimensional imaging may provide a quantitative assessment of volume changes in various diseases such as kidney, liver, and spinal cord injury models. Therefore, OCT stand for an exciting new approach to visualize, in real-time, the pathological changes in the living organs in a minimally invasive fashion (9). In this context, OCT will be a promising imaging modality to assess tissue pathologies in situ and in real time. (10).

1.1 Overview

1.1.1 Overview of tissue imaging techniques based on light microscopy

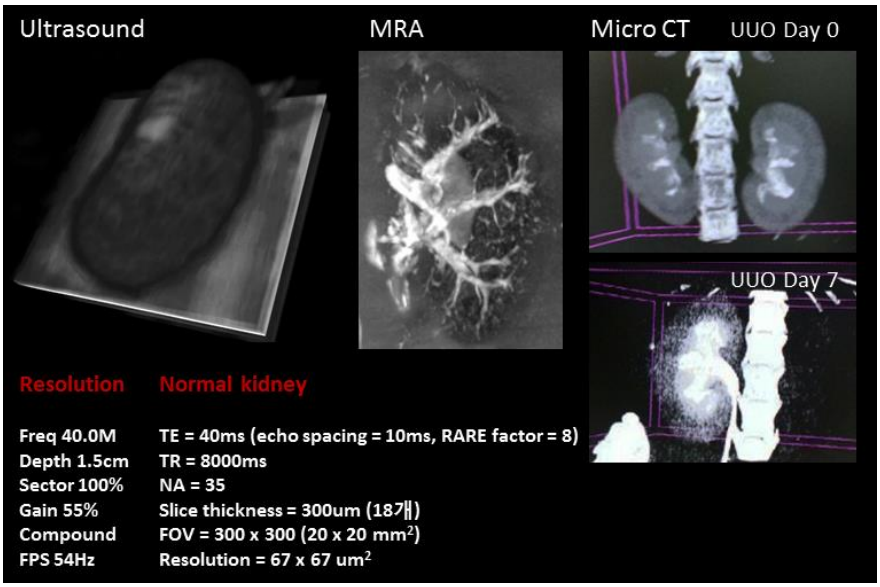

Figure 1-2. Comparative study of imaging modality. Ultrasound, MRA, CT images from left, respectively.

Imaging devices that visualize these blood vessels in a macroscopic manner exist CT and MRI using contrast agents. They have an excellent advantage of getting a whole image from human and animal organs. However, there is a disadvantage that it is difficult to obtain precise images if the absorption of the contrast agent is not smooth due to the damage of the blood vessels. It is nice to observe the whole image with the image quality that can reach the maximum. However, the structure and function of cells connections and organs remain a large-scale study. Conversely, microscopic imaging modalities include confocal laser scanning microscopy and two-photon excitation microscopy. These are imaging devices that utilize light scattering and absorption. Because the image depth is as small as a few hundred microns, cell networking studies are possible, but cannot be extended to large-scale organ functional or structural studies. So that, imaging gaps remain between these macroscopic and microscopic tools, and these differences are still emerging in the study of anatomy and pathology.

1.1.2 Optical imaging for blood vessel network research

Imaging of the blood vessel lumen can be best acquired by injecting a contrast agents into the vessel and then imaging the agents with X-ray, CT, or MR technologies, but a lot of information can be disappeared by measuring flow through the vessels with ultrasound. Because of the increased risk of stroke with conventional angiography, CT angiography or MR angiography is often the first choice of enquiring for imaging intracranial arteries, but doppler ultrasound is still frequently used to assess the carotid arteries. Interpreting the results from any modality requires a good knowledge of vessel anatomy

(11). Doppler OCT is an imaging technique using optical coherence tomography. The noninvasive characteristic and exceptionally high spatial resolution of ODT have many powerful applications in the clinical trial of patients in whom imaging tissue morphological structure and monitoring blood-flow dynamics are essential (2).

1.1.3 Optical coherence tomography: Organ imaging using tissue clearing method

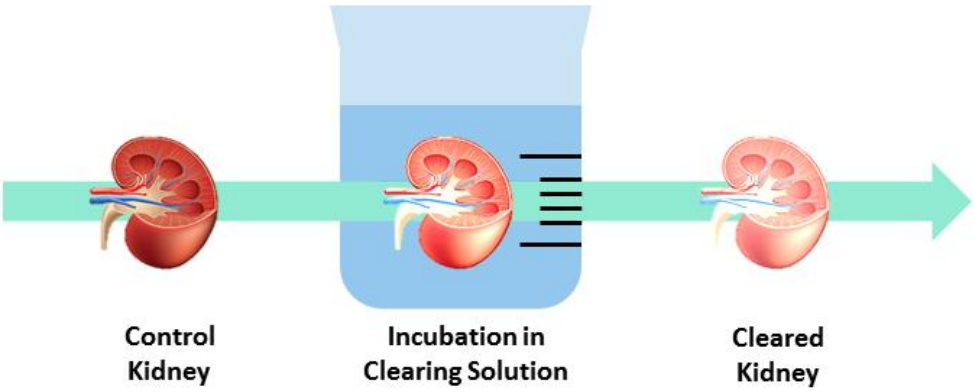

Figure 1-3. Tissue clearing by refractive index matching. Because of the reflection coefficient is proportional to refractive index gap, index matching reduces light scattering.

Optimum tissue clearing is necessary for OCT imaging contrast, and this is because OCT imaging contrast based on the scattering. To increase the imaging depth tissue clearing is essential. However, imaging contrast tends to be reduced. Therefore, we have to optimize the tissue clearing by considering imaging contrast and imaging depth. We compared the OCT depth profile according to various clearing technique and monitored the OCT depth profile depending upon a time. By analysis of OCT depth profile, we find out the optimal tissue clearing for OCT imaging. Moreover, for future works in situ experiment, development of biodegradable clearing solution is demanding without any fatal harm (12). The method of hydrolysis by electrophoresis, the passivation method which removes lipid by passive penetration, the method of removing lipid by the organic solvent, the method of transparency of tissue which is the most preferred of OCT by hyper-hydration method is a method of hydrolysis. So we use the Scale method. Among the major components of the scale solution, both urea and sorbitol have tissue-clearing properties, but urea causes hydration, resulting in tissue expansion, whereas sorbitol causes dehydration, leading to tissue contraction. By controlling the concentration ratio of each component, we were able to obtain tissue clearing while preserving the original sample volume, although there were the expansion and shrinkage phase. Glycerol could further counterbalance the urea-induced tissue expansion and promote further dehydration; sorbitol is hydrophilic, but glycerol is amphipathic and is predicted to target lipophilic tissue regions (13).

Chapter 2. Experimental methods and materials

2.1 Optical coherence tomography

2.1.1 Optical coherence tomography set-up

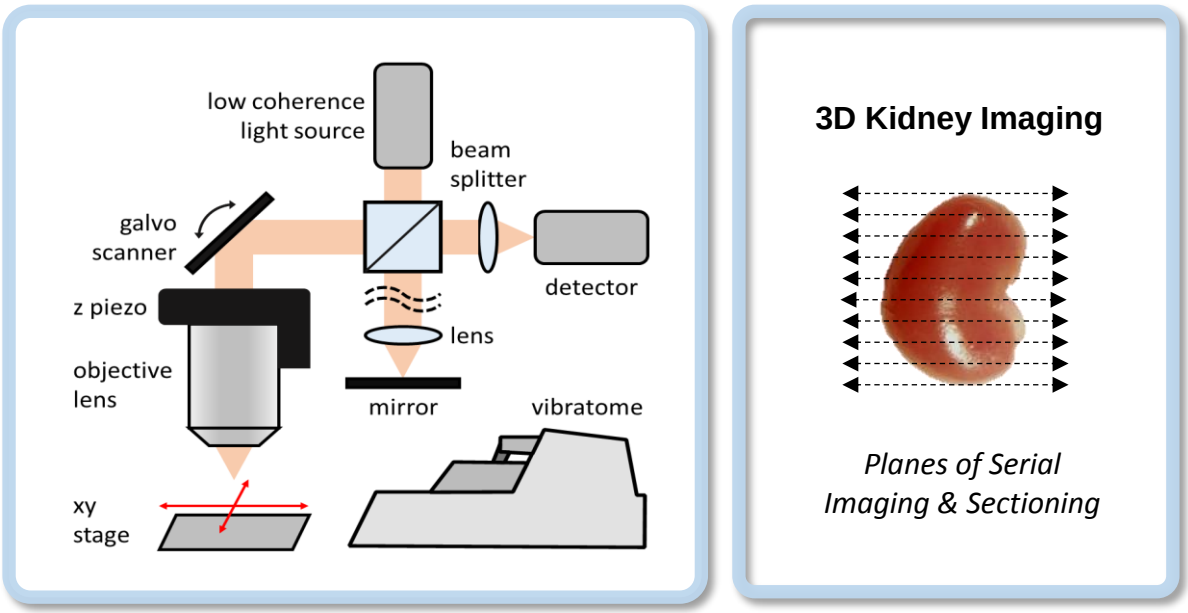

Figure 2-1. Schematics of serial OCT (SOCT) and sectioning directions. (Transverse way)

As shown in Fig 2-1, spectral domain optical coherence tomography (SD-OCT) that enables 3D OCT imaging used in this study (14). SD-OCT system incorporates laser output generated by a super luminescent light emitting diode (SLD, EXS210004-02, Exalos, USA) with a center wavelength of 1310nm and a bandwidth of 80nm based on Michelson interferometer (15). The light beam was split at beam splitter by 50:50 and moved toward reference and sample arms. The back-reflected lights from both arms are recombined at the beam splitter and travel towards a detector which incorporates a spectrometer containing diffraction grating (Wasatch Photonics 1145 lines/mm), and an achromatic doublet lenses (Thorlabs, USA) (16). At detector, a 12- bit InGaAs CMOS camera (SU-1024LDM, SUI Goodrich, USA) with 1024 pixels array connected with a frame grabber (PCIe-1429; National Instruments, USA) is employed to acquire the interference fringes. Two galvano-scanners (Thorlabs, USA) are driven by a DAQ board (National Instruments, USA) to perform three-dimensional scanning. Eventually, detected fringe signals by CCD are passed into the computer having Core i7-processor, 32 GB RAM and NVIDIA GTX 970 graphic card for processing.

2.1.2 Serial optical coherence tomography imaging

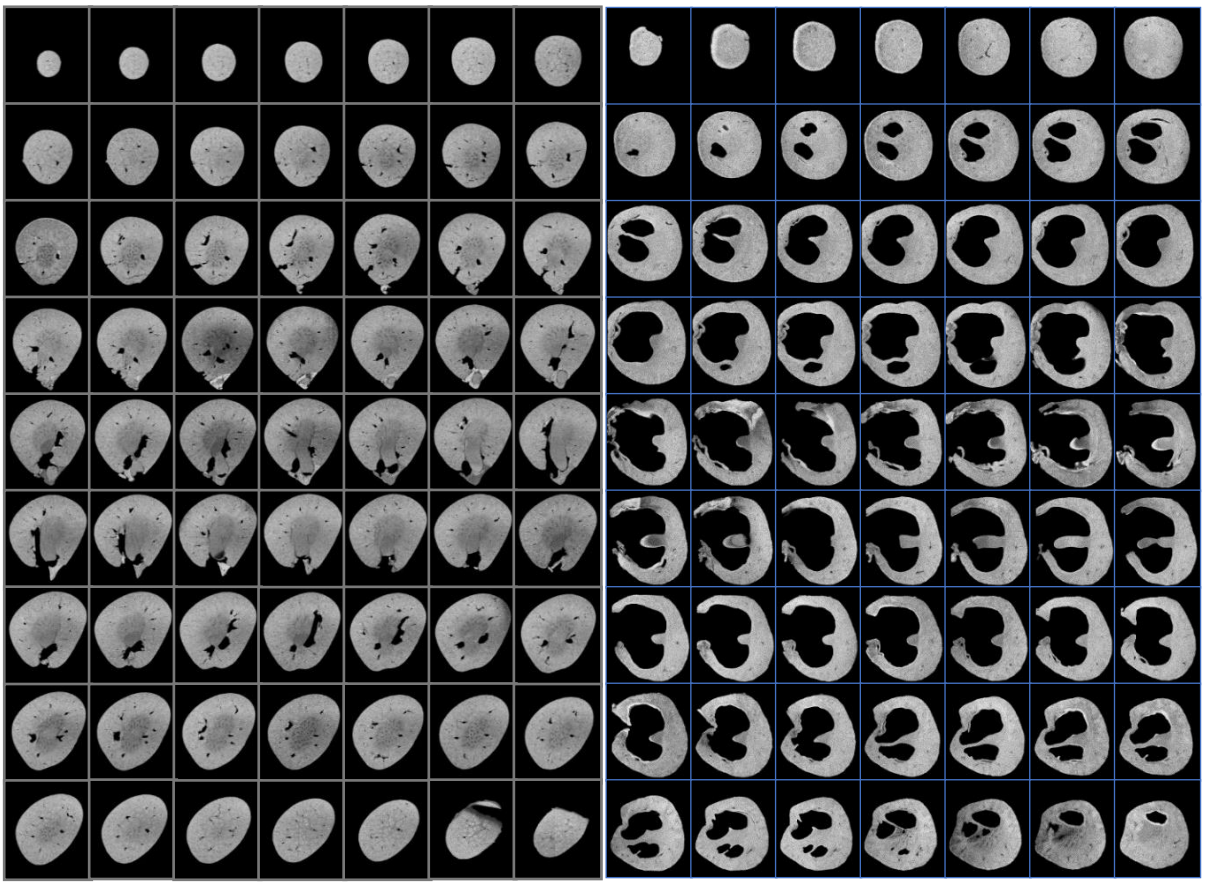

Figure 2-2. Imaging of the entire kidney by using serial sectioning method. By sectioning 200um with a normal and disease induced model.

For continuous imaging, the following steps are required: First of all, it is the calibration of pixel resolutions. When we obtained the images, we always adjusted the axial and lateral pixel resolution. For the axial calibration, we prepared a tissue slice of known thickness using a vibratome then imaged tissue. Since the axial resolution significantly depends on the refractive index of imaging tissues, we used the sample slice of known thickness when we measured the axial pixel resolution to calibrate it.

Then sample embedded in agarose gel to avoid deformations is mounted and attached to a rotation/translation platform for precise positioning of the sample in three dimensions (17). XY-galvanometer scans transversely sectioned kidney block face submerged in water. In order to make the flat surface of kidney as required for optimal OCT acquisition, kidney specimen has been sliced by a freezing sliding vibratome with the thickness of 200 um until it is completely imaged from top to bottom in transverse way. A series of flat-facing process generated an extremely flat surrounding for the tissue which help enhance the data acquired with OCT, by giving a homogeneous illumination evenly when the surface is focused by light in sample unit. Generally, we sectioned sixty tree slices at 200 um of each case as shown in figure 2-2 above, and each data acquisition consisted of a 3D volume.

2.1.3 Optical coherence microscopy

2.2 Tissue preparation

2.2.1 Animal preparation

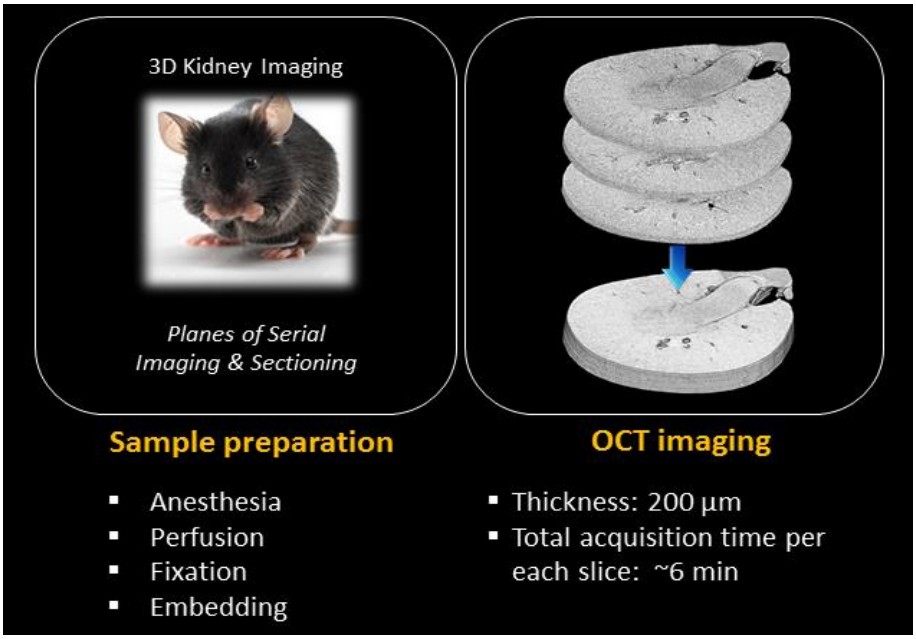

Figure 2-3. Biological sample preparation and SOCT imaging. C57BL/6 8weeks male mice were used (left). And we imaged the tomographic image into a blocks.

By using eight weeks C57BL/6 male mice, our experiments performed. The studies approved by the Ulsan National Institute of Science and Technology, IACUC, Animal Care and Use Committee. Each animal group consisted of at least five mice. The mice sacrificed with Zoletil/Rompun mixture (40 mg/kg body ip) then kidneys were both perfusion-fixed in PBS and 10% Neutral Buffered Formalin (Sigma) for histological studies and frozen in liquid nitrogen for biochemical studies (18).

2.2.2 Surgical procedure

Chronic Kidney Disease: Unilateral Ureter Obstruction

The mice were anesthetized with Zoletil/Rompun mixture (0.8mg/kg body ip; catalog no.). After a haircut, right kidney exposed through the site of the right flank incision (19). The right ureter was obstructed completely near the renal pelvis using a Black 6.0 silk tie. Sham-operated mice underwent the same surgical procedure except for the ureter ligation. The mice sacrificed at 0, 3, 5, seven days after the procedure for a dynamic progression of CKD injury.

Acute Kidney Injury: Ischemia/Reperfusion Injury

The mice were anesthetized with Zoletil and Rompun mixture (0.8mg/kg body ip; catalog no.). After a

haircut, right kidney exposed through the site of the right flank incision. Ischemia/reperfusion injury induced for 30 min by clamping renal pedicle with non-traumatic microaneurysm clamp (Roboz Surgical Instruments, Washington, DC) (20). When clamp removed, reperfusion was confirmed completely. Then, Sham-operated mice underwent the same surgical procedure except for the renal pedicle clamping. And the mice were sacrificed at 0, 1, 3, 5, seven days after the procedure for a dynamic progression of I/R injury.

2.2.3 Fixation and clearing method

Histology

Tissues were harvested and flow through with PBS then fixed with 10% Neutral buffered formalin (NBF). After washed with PBS three times for 5 min each, tissue processor procedure was conducted for embedded in paraffin at room temperature and then cut into 4-μm paraffin sections using a microtome (catalog no. RM2165; Leica) (21). Sections of kidney tissue were stained with routine hematoxylin and eosin (H&E) or Immunohistochemistry (22). By using the .slide (Dot slide, Olympus Upright Microscope BX51), we could get the denser light microscope photographs. Also, with Laser Scanning Confocal Microscopy (FV1000, Olympus motorized inverted microscope IX81), we could acquire the finer fluorescence images.

Tissue Clearing

Among the major components of the scale solution, both urea and sorbitol have tissue-clearing properties, but urea causes hydration, resulting in tissue expansion, whereas sorbitol causes dehydration, leading to tissue contraction. By controlling the concentration ratio of each component, we were able to obtain tissue clearing while preserving the original sample volume, although there were the expansion and shrinkage phase. Glycerol could further counterbalance the urea-induced tissue expansion and promote further dehydration; sorbitol is hydrophilic, but glycerol is amphipathic and is predicted to target lipophilic tissue regions (13).

Renal functional parameter for creatinine measurement

Mouse blood samples were gathered from the retro-orbital venous plexus. By using Creatinine Assay Kit (Abnova, KA0849) we can take a Plasma creatinine numerical values.

2.3 Image processing

2.3.1 Image processing for OCT analysis

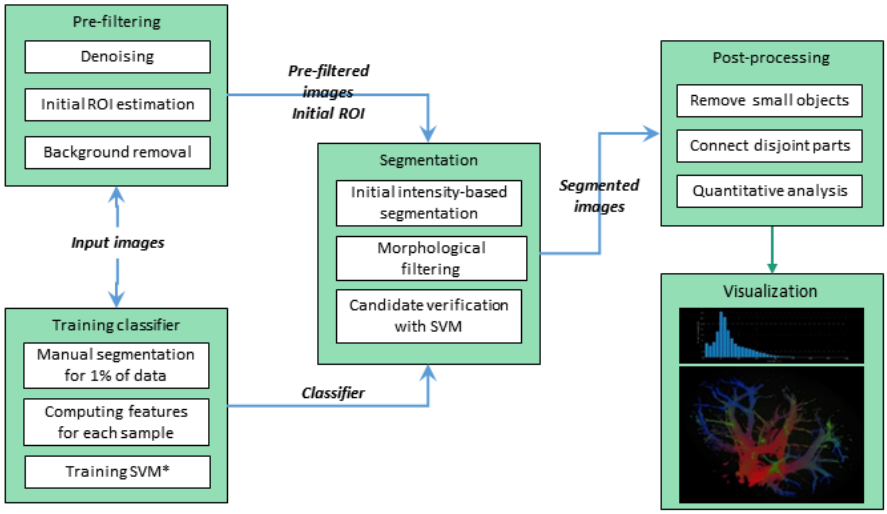

Figure 2-4. Home built image processing system.

Home built OCT system achieves cross-sectional images (B-scans) of bio-sample with an axial and lateral resolution of 10um. A stack of consecutive B-scan images is converted to enface images from which 3D volume of a single optical section is acquired. The mouse kidney sample was sliced with a thickness of 200 um through vibratome and scanned sequentially until the entire kidney is imaged. All sections are aligned along the z-direction and merged together to reconstruct the whole volume of mouse kidney in 3D. Image processing method starts with filtering operations used to remove noise and correct intensity attenuation. Then b-scans are converted into en-face images and adaptive background removal algorithm is used. Global intensity correction is applied to eliminate brightness inconsistency between sections. Filtered images are passed to segmentation step. In proposed method, blood vessel and UUO hole are segmented in parallel. Blood vessel segmentation utilizes Support Vector Machine (SVM) algorithm. It requires manual selection of blood vessels in 1% of *enface* images in the dataset. Based on manually selected positive samples and automatically selected negative samples from same images, the classifier is trained and applied to remained images. Small discontinuities in the blood vessel network are fixed using curve fitting. As a result, 3D structure showing the probability of blood vessel to be presented in every voxel is obtained. Empty hole segmentation starts with an automatic selection of initial image according to the following criteria: this image should have high contrast and brightness, and biggest area of the hole, segmented by Otsu's method. This hole is then traced though the whole image stack. Obtained structure is smoothed with interpolation. Segmentation results are combined with reconstructed blood vessel structure. Overlapped regions are corrected based structural information. Finally, data is processed to remove small objects. Obtained data is analyzed to get quantitative parameters, such as the volume of a hole, length and radius of blood vessels, volume of the whole kidney.

Chapter 3. Result

3.1 Volumetric optical kidney imaging

3.1.1 Morphological changes with normal and diseased model

In figure 3-1 shows Serial sectioning OCT system in spectral domain produces the 2D tomographic image based on Michaelson interferometer using the light source of having the center wavelength of 1310 nm in near infrared region. The 4x lens was adopted in sample unit, and vibratome has been implemented for accurate serial sectioning, which is collected as constructing the 3D volumetric image. Scanning range was determined to the degree which the spatial resolution can be maintained. Specifically for the transverse resolution to be maintained in 10 um, pixel resolution has also been considered to be 5 um/pixel, resulting from the number of A-mode of 1600 in scanning 8 mm of kidney slice. In order to know the performance of developed serially sectioning spectral domain OCT, we were imaging from normal one. 8 weeks-old mouse was sacrificed, and kidney was extracted after fixation process. The fixed kidney was embedded in the agarose gel so that the vibratome could remain vertical when cutting the blocks. The sample was sectioned in a transverse way with the thickness of 170um. And we visualized a normal kidney in all directions; sagittal, coronal, and transverse (Fig 3-1). In the direction of transverse, the direction of movement of the vessel can be observed more clearly when the movement of the vessel is moved in a different direction. And in the direction of coronal, we were able to observe the inner morphology of the kidney tubules and glomeruli as accurately as the biopsy. One of the strong advantages of OCT, which is deep penetration depth, efficiently enables to have the 3D reconstruction of renal morphology because it reduces the total sectioning number and time. Compared with the same case using histology sectioning in the thickness of 4um in general, serial sectioning OCT gives users way easier access to reconstruct 3D volumetric images in relatively short time. The UO, a model of our CKD model, is caused by blockage of urinary track. And the pressure of the urine pushes the blood vessels and other inner components of the kidney, causing tissue damage to the whole kidney primarily inner medulla and the outer medulla. When the disease progressed to a total of 7 days, most of the internal tissues were moved to the cortex region and found to compress on the 7th day. Seven days later, we harvested kidneys and visualized by using OCT and histology, respectively. As shown in Figure 3-2 Particularly, images taken with OCT can image the size of empty holes separately for the whole kidney volume and quantitatively analyze the ratio. The plot is to show the ratio of empty hole volume to its entire volume. And the ratio is increasing and hit the highest value in 7 day of UUO case as expected (Fig 3-2). Quantification of the empty cavity allows us to quantify and analyze the extent of disease progression, as well as provide the ratio of total kidney and inner components to optical histopathological data.

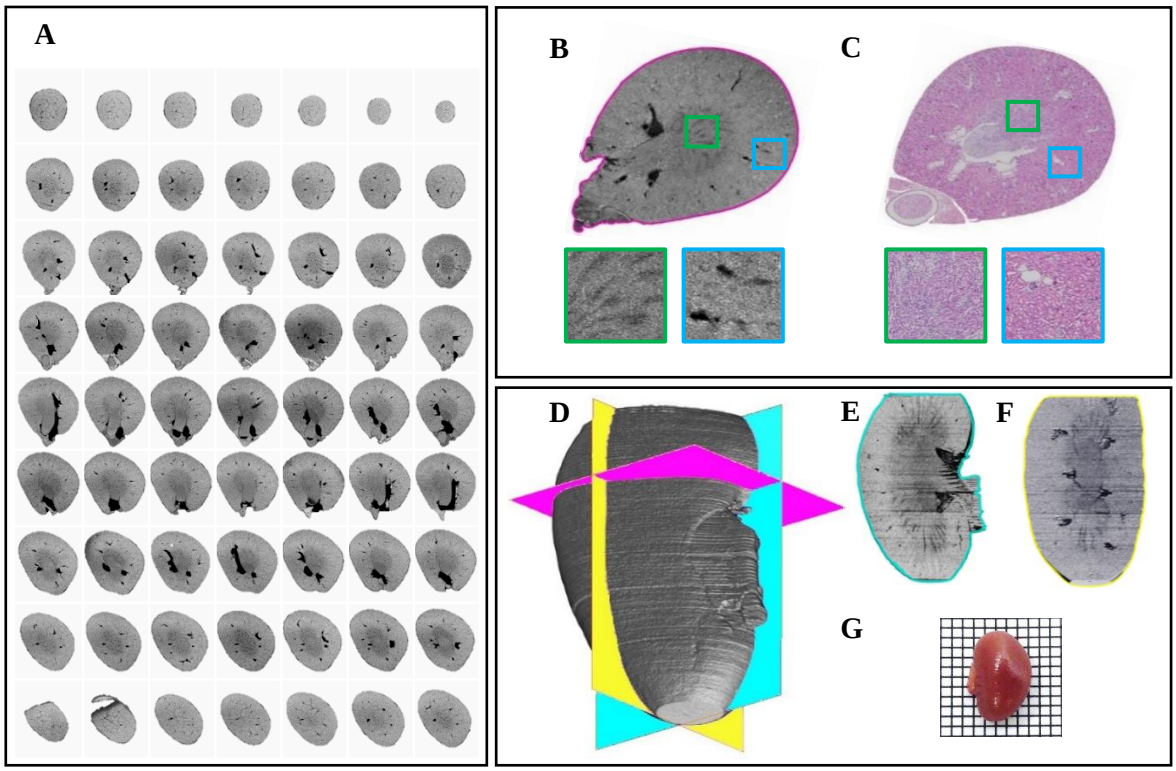

Figure 3- 2. Serial sectioning spectral domain OCT (SD-OCT) system. (A) 200um of the sectioning slices. (B, C) Correlation study of OCT vs. Histology (4X image). (D, E, F) Various sectioning directions. (G) Actual size of kidney (8mm x 12mm)

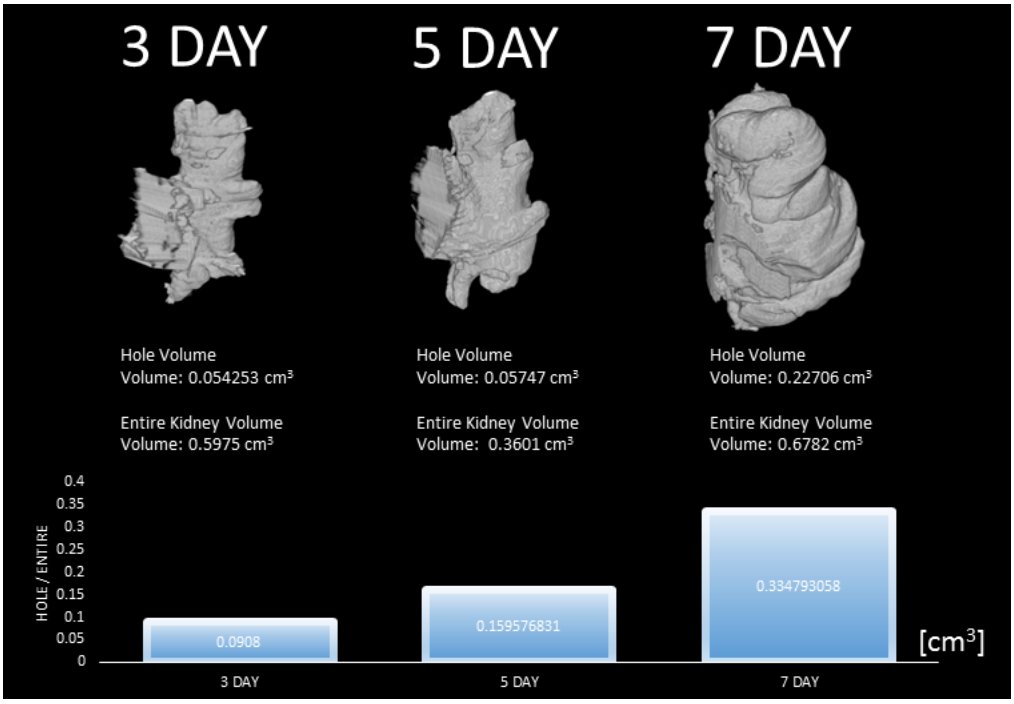

Figure 3- 1. Quantify the total volume of empty holes. It is possible to quantify the increase in the volume of the empty hole from 3 to 7 days

3.1.2 Comparison study: OCM, Histology and Immunohistochemistry

In figure 3-2, using the OCM system, we can verify that images similar to organizational inspections can be acquired at the same scale and the same image quality was demonstrated without having to any staining method. And OCT image comparing with H&E histology, pelvic wall, inner/outer medulla can be seen as clear as H&E histology. Moreover, H&E histology, one of golden standards in kidney study for finer confirmation, has been compared with the OCM image about the similar area in same magnification by switching the magnification of objective lens in sample arm with higher one. Using mosaic techniques, it accomplished to have the larger area of scanning range over the entire kidney slice sectioned in a coronal way. In a result, by knowing its total number, shape, and pattern depending on disease level, we were able to predict its degree of renal function failure. For the accurate comparison, we compared OCM image with H&E histology in same magnification of the 20x lens. The specimen this time was sectioned in a coronal way. Then we marked three area by the square box where the characteristic of each region can be defined very easily. At the same magnification as the OCT and histology, there was no loss of information, and when the three points were enlarged for more precise viewing, the same information could be given at the same site. However, since OCM did not stain with a particular dye, information on the nuclei could not be given for reasons similar to the surrounding tissue. In Fig 3-2. As shown in box a, it is major calyx part. In this section of the kidney, it was visualized that there are not as many of tubules as in cortex region. In box b of Fig 3-3, it is showing a boundary region between outer medulla and cortex. Fibrous zone of upper left corner shows different texture in comparison with tiny tubules of the lower right corner (Fig 3-3. c). For the comparative study of OCT and histology, we did routine H&E as well as fluorescent staining (Fig 3-4). We used Dapi to stain the whole nucleus and used the collagen-1 antibody to capture the fibroblast and to obtain the vascular information we use α-smooth muscle antibody. Through this study, it became apparent that OCM has the unique contrast to study macroscopic renal structures, especially in glomeruli and vessels.

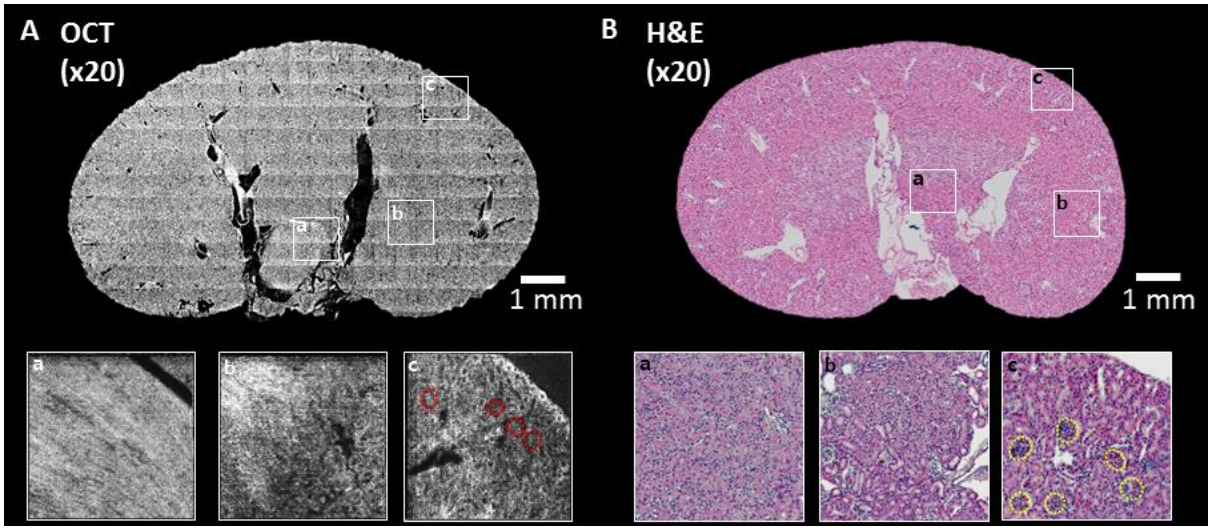

Figure 3- 3. Comparison study: OCM, Histology. (A) 20X OCM image. a: major calyx, b: inner medulla, c: cortex area. (B) 20X Histology image. Imaging the same location as the OCM

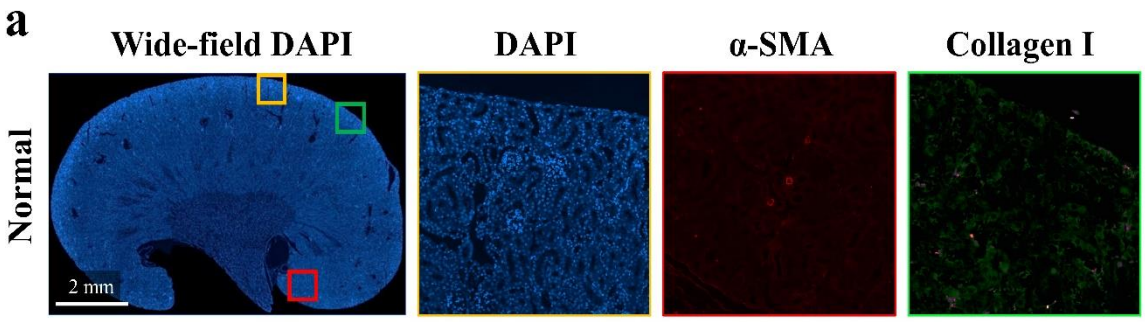

Figure 3- 4. Area fraction in renal morphology. (a) Immunohistochemistry of DAPI in wide field, and magnified cortex region of DAPI, α-SMA, and collagen I in time scale of AKI.

3.1.3 Blood vessel network normal and diseased model

Since before starting to image the kidney slice, the sample was properly perfused out, so that any capillaries across all the tissues delivering blood has changed to be hollow. So there would be no scattering effect on each vessel, making it be visualized in dark. This contrast difference between blood vessels and surrounding tissues make the huge benefit to the user using the OCT because it illustrates entire blood vessel network in micro-scale as shown in Fig 3-5. Spectral Domain OCT is the optimized tool to have entire whole kidney and blood vessel network visualized in three dimensions. The blood vessel has been hollow due to perfusion, so each dark hole across the OCT kidney image represents vessels without blood. Kidney blood vessel architecture reconstructed from day 0 to day 7 of unilateral ureter obstruction. Sectioning thickness was 200um each in both cases. Kidney was filled with urine and swollen before it was extracted out of mouse body. UUO model compared with Normal one, it shows a tendency that blood vessel was pushed to outer part of cortex and the density of blood vessel are way more reduced from normal model. In Fig 3-6. It is the blood vessel up to 3rd order which is being used as a marker of our quantification data. And volume computation of each empty hole as well as its entire kidney of disease model of UUO has been performed as stage of disease is getting worse. In Fig 3-7, the volume of each part of kidney has been calculated quantitatively. The skin color is representing entire kidney, red one is blood vessel, and the gray one is empty hole created by UUO damage. It shows a tendency that the blood vessels is decreasing while the volume of empty hole is increasing as the stage of UUO is developing in time basis. (Figure 3-8) Furthermore, using these advantages, we need to study images to study the kidney function in the disease model. As shown in Figure 3-9, In order for glomeruli to be examined, we developed our system capable of providing axial information up to several hundred micron under the tissue without any labelling, showing different shapes of tubules and glomeruli with entire 3D renal morphology.

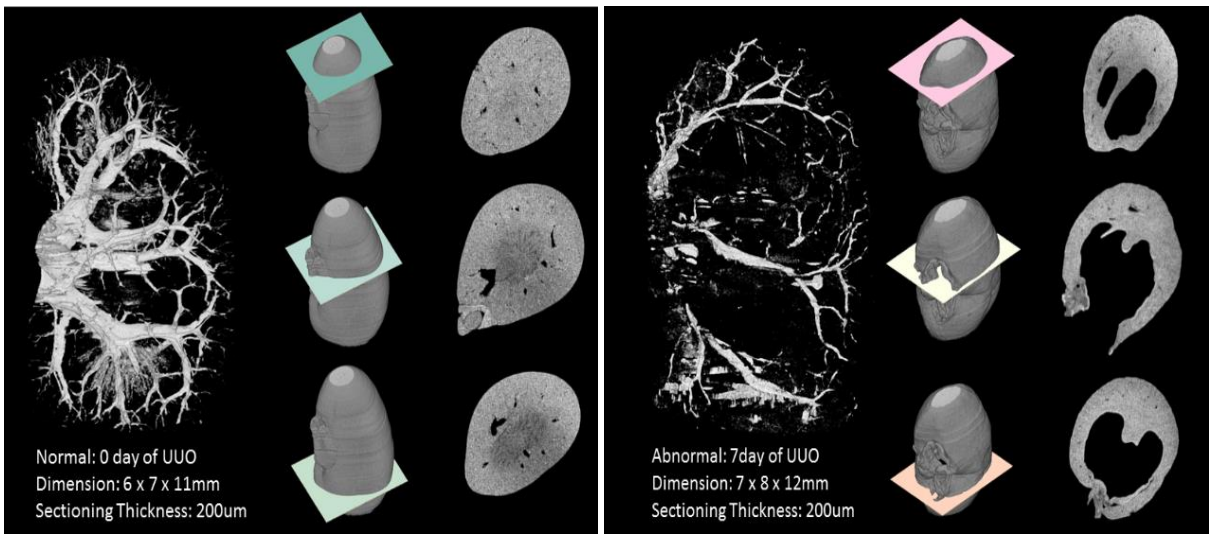

Figure 3- 5. Renal blood vessel architecture reconstructed from day 0 to 7 of CKD model (Unilateral Ureter Obstruction)

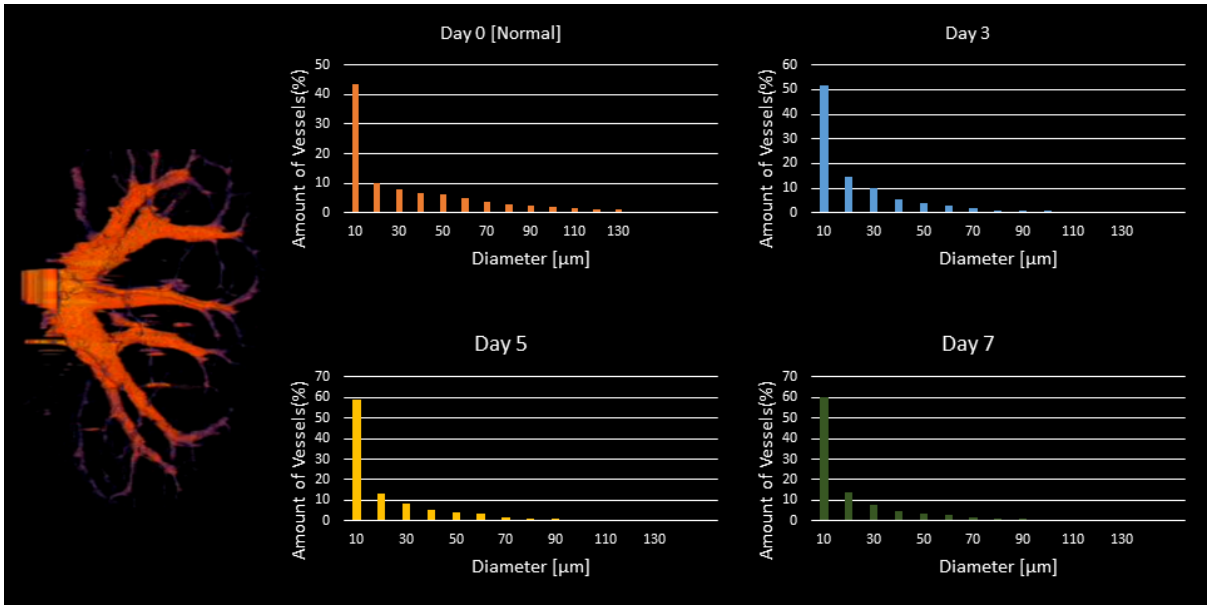

Figure 3- 6. Renal blood vessel quantification from day 0 to 7 of CKD model (Unilateral Ureter Obstruction)

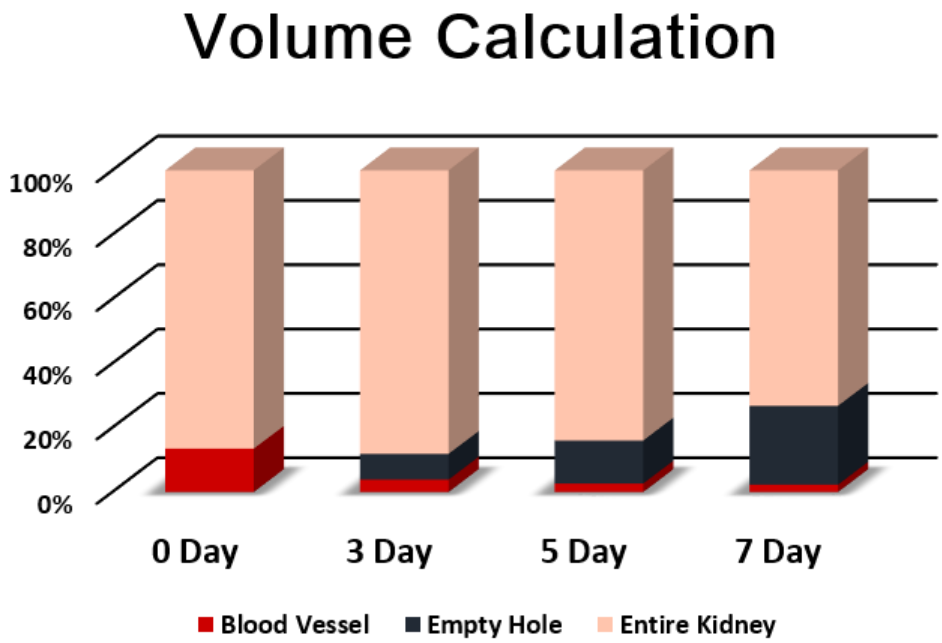

Figure 3- 7. The volumetric information of each part of kidney.

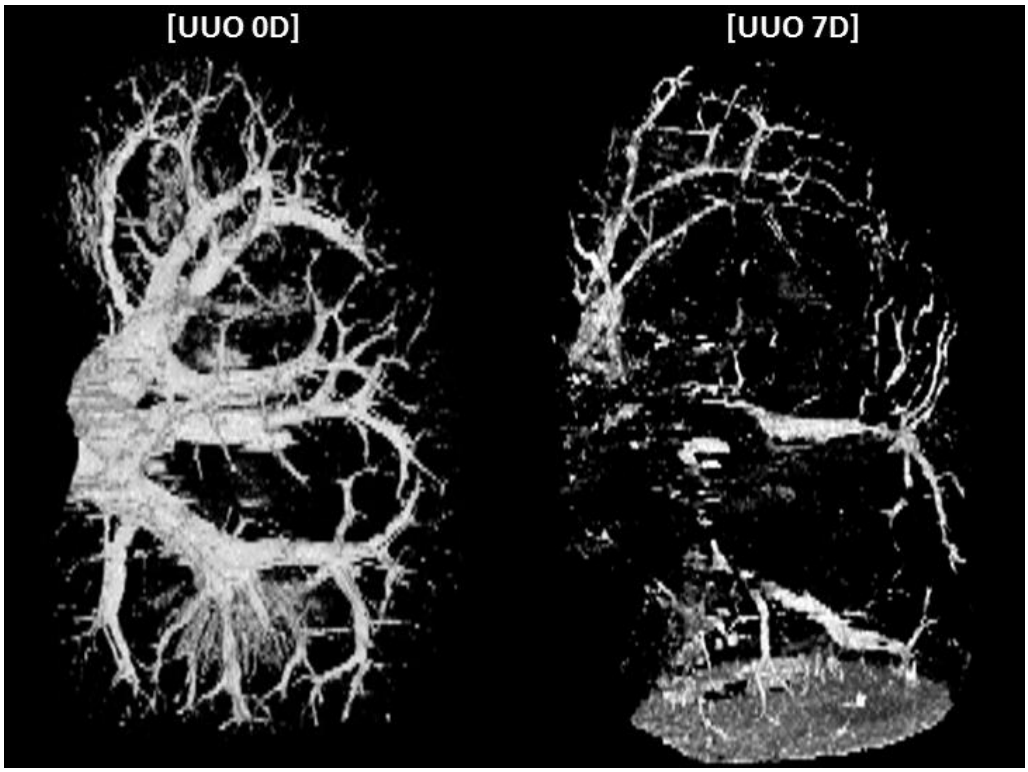

Figure 3- 8. Renal vessel reconstruction of normal and disease models. We obtained both renal volumetric structure and blood vessel network.

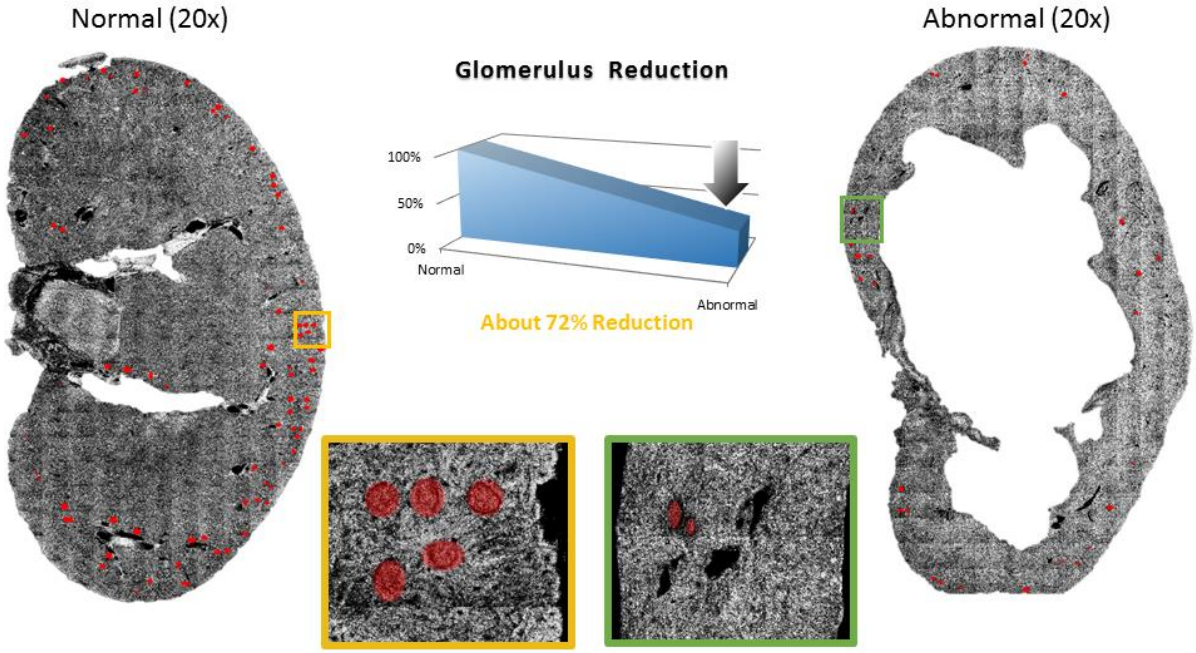

Figure 3- 9. Glomerulus of normal and disease models. A graph showing the number of glomeruli and its shape in the normal and diseased models of the kidneys.

4. Discussion

4.1 Expanded application Study

4.1.1 Spinal cord, Liver and Skin

We have been able to test the potential function of the serial OCT by reconstruct the morphology of the kidney in the studies described earlier. Figure 4.1 we applied it to 3D Serial OCT images of mouse spinal cord, liver, and skin. Since the intensity of the fiber absorbed by the spinal cord was greater than 150 μm compared to the spinal cord, the thickness of the skin was reduced to 100 μm.

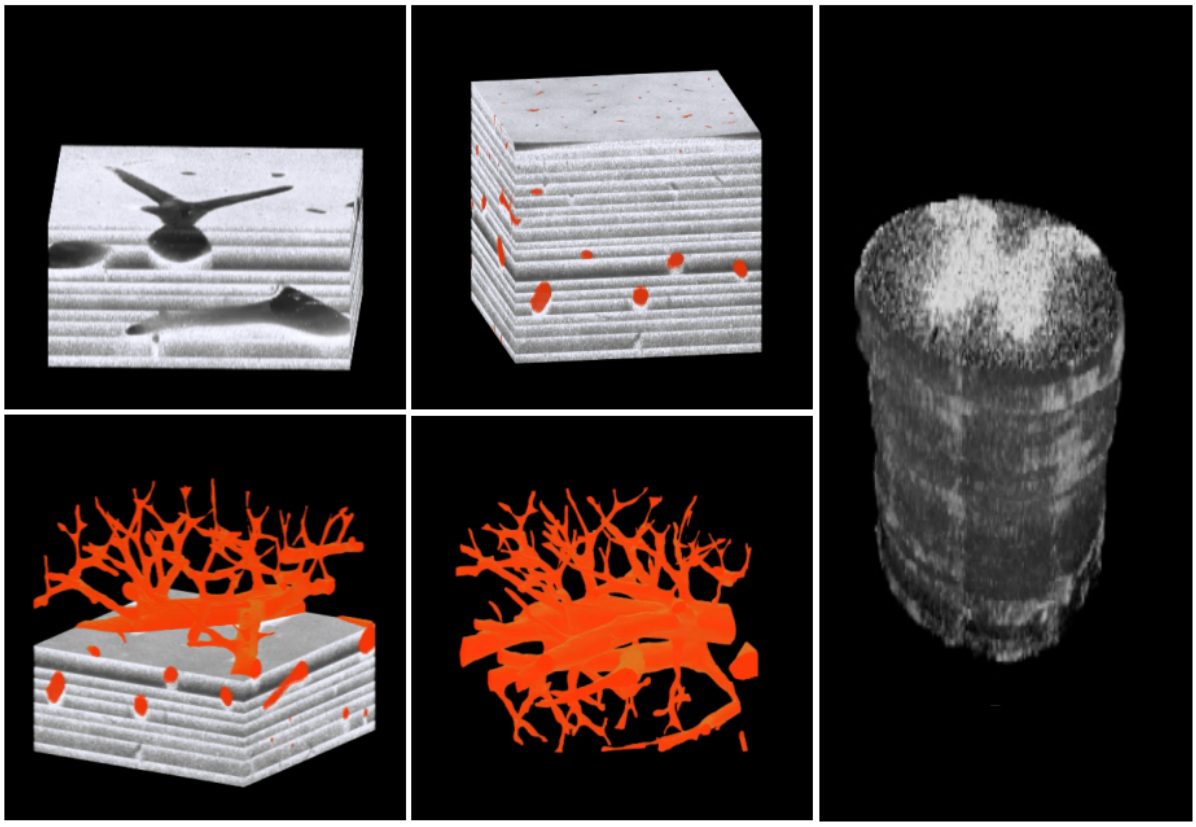

Figure 4-1. 3-dimensinal organ reconstruction. Through 3D reconstruction, we can obtain liver and spinal cord as much as we would like to see.

4.1.2 Tissue Transparency for Optical Coherence Tomography

By using tissue clearing methods, we can adjust the transparency of organs to better penetrate depth the organs and achieve higher resolution data than normal steady-state. Also, we use the scale method described in chapter 1.1.3, we will be able to perform long-term tracking with 3-D optical tomography images by implanting a window into the spinal cord injury model using a bio comparable solution in the in-vivo state.

5. Conclusion

In this study, we introduced a new capable method of serial sectioning microscopy, named Serial OCT. By using our method, we can visualized the whole structure of mouse kidney, spinal cord, liver and so on. To obtain the advantageous contrast and resolution of Serial OCT imaging, we studied to compare with the contrasts of other imaging technique such as histology as well as the resolutions obtained with high-magnification objective lenses. Thus, we conclude that Serial OCT imaging has great contrast on renal structures equal with both glomeruli and lots of tubules. And also vasculature as well as great resolution sufficient to visualize fine renal structures. Through image processing, we extracted the 3D structure of vessels network. In addition, we quantitatively measured the volumes of these structures. Therefore, we demonstrated that Serial OCT may be used for studies that provide both morphological and pathological information at the same time.

Reference

1. Risau W. Mechanisms of angiogenesis. Nature. 1997;386(6626):671.
2. Zhao Y, Chen Z, Saxer C, Xiang S, de Boer JF, Nelson JS. Phase-resolved optical coherence tomography and optical Doppler tomography for imaging blood flow in human skin with fast scanning speed and high velocity sensitivity. Optics letters. 2000;25(2):114-6.
3. Bonventre JV. Mechanisms of ischemic acute renal failure. Kidney Int. 1993;43(5):1160-78.
4. Kim J, Jang HS, Park KM. Reactive oxygen species generated by renal ischemia and reperfusion trigger protection against subsequent renal ischemia and reperfusion injury in mice. Am J Physiol Renal Physiol. 2010;298(1):F158-66.
5. Tian J, Varga B, Somfai GM, Lee W-H, Smiddy WE, DeBuc DC. Real-time automatic segmentation of optical coherence tomography volume data of the macular region. PloS one. 2015;10(8):e0133908.
6. Wang LV, Hu S. Photoacoustic tomography: in vivo imaging from organelles to organs. Science. 2012;335(6075):1458-62.
7. Huang D, Swanson EA, Lin CP, Schuman JS, Stinson WG, Chang W, et al. Optical coherence tomography. Science (New York, NY). 1991;254(5035):1178.
8. Jang I, Bouma B, MacNeill B, Takano M, Shishkov M, Iftima N, et al., editors. In-vivo coronary plaque characteristics in patients with various clinical presentations using Optical Coherence Tomography. Circulation; 2003: LIPPINCOTT WILLIAMS & WILKINS 530 WALNUT ST, PHILADELPHIA, PA 19106-3621 USA.
9. Chen Y, Aguirre A, Hsiung P-L, Desai S, Herz P, Pedrosa M, et al. Ultrahigh resolution optical coherence tomography of Barrett's esophagus: preliminary descriptive clinical study correlating images with histology. Endoscopy. 2007;39(07):599-605.
10. Regatieri CV, Branchini L, Fujimoto JG, Duker JS. Choroidal imaging using spectral-domain optical coherence tomography. Retina (Philadelphia, Pa). 2012;32(5):865.
11. Rana AQ, Zumo LA, Sim V. Blood Vessel Imaging. Neuroradiology in Clinical Practice. Cham: Springer International Publishing; 2013. p. 93-8.
12. Richardson DS, Lichtman JW. Clarifying tissue clearing. Cell. 2015;162(2):246-57.
13. Hama H, Hioki H, Namiki K, Hoshida T, Kurokawa H, Ishidate F, et al. ScaleS: an optical clearing palette for biological imaging. Nature neuroscience. 2015;18(10):1518-29.
14. Chaikitmongkol V, Durbin M, Bressler S, Bressler N. Assessment of Cirrus™ OCT Registration in Macular Edema from Diabetes or Retinal Vein Occlusion. Investigative Ophthalmology & Visual Science. 2013;54(15):3617-.
15. Wang Y, Tan O, Huang D, editors. In vivo retinal blood flow measurement by Fourier domain

Doppler optical coherence tomography. Biomedical Optics (BiOS) 2008; 2008: International Society for Optics and Photonics.

16. Hou R, Le T, Murgu SD, Chen Z, Brenner M. Recent advances in optical coherence tomography for the diagnoses of lung disorders. Expert review of respiratory medicine. 2011;5(5):711-24.

17. Arranz A, Dong D, Zhu S, Rudin M, Tsatsanis C, Tian J, et al. Helical optical projection tomography. Optics express. 2013;21(22):25912-25.

18. Kim J, Padanilam BJ. Loss of poly (ADP-ribose) polymerase 1 attenuates renal fibrosis and inflammation during unilateral ureteral obstruction. American Journal of Physiology-Renal Physiology. 2011;301(2):F450-F9.

19. Cho MH, Jang HS, Jung KJ, Park KM. 17beta-estradiol Attenuates Renal Fibrosis in Mice with Obstructive Uropathy. Journal of the Korean Society of Pediatric Nephrology. 2011;15(2):125-

20. Jang H-S, Kim J, Kim KY, Kim JI, Cho MH, Park KM. Previous ischemia and reperfusion injury results in resistance of the kidney against subsequent ischemia and reperfusion insult in mice; a role for the Akt signal pathway. Nephrology Dialysis Transplantation. 2012;27(10):3762-70.

21. Kim J, Park J-W, Park KM. Increased superoxide formation induced by irradiation preconditioning triggers kidney resistance to ischemia-reperfusion injury in mice. American Journal of Physiology-Renal Physiology. 2009;296(5):F1202-F11.

22. Ko GJ, Boo C-S, Jo S-K, Cho WY, Kim HK. Macrophages contribute to the development of renal fibrosis following ischaemia/reperfusion-induced acute kidney injury. Nephrology Dialysis Transplantation. 2007;23(3):842-52.